Defence Science Journal, Vol. 62, No. 6, November 2012, pp. 382-389, DOI: 10.14429/dsj.62.2666

Ballistic Studies on TiB_2-*Ti* Functionally Graded Armor Ceramics

Neha Gupta[*], V.V. Bhanu Prasad[#], V. Madhu[#], and Bikramjit Basu[*,!]

[*]*Indian Institute of Technology Kanpur, Kanpur- 208016, India*
[#]*Defence Metallurgical Research Laboratory, Hyderabad- 500058, India*
[!]*Indian Institute of Science (IISc), Bangalore-560012, India*
[*]*E-mail: nehgupta@iitk.ac.in*

ABSTRACT

The objective of this paper is to discuss the results of the ballistic testing of spark plasma sintered TiB_2-*Ti* based functionally graded materials (FGMs) with an aim to assess their performance in defeating small-calibre armor piercing projectiles. We studied the efficacy of FGM design and compared its ballistic properties with those of TiB_2-based composites as well as other competing ceramic armors. The ballistic properties are critically analyzed in terms of depth of penetration, ballistic efficiency, fractographs of fractured surfaces as well as quantification of the shattered ceramic fragments. It was found that all the investigated ceramic compositions exhibit ballistic efficiency (η) of 5.1 -5.9. We also found that by increasing the thickness of FGM from 5 mm to 7.8 mm, the ballistic property of the composite degraded. Also, the strength of the ceramic compositions studied is sufficient to completely fracture the nose of the pointed projectile used. Analysis of the ceramic fragments (2 μm-10 mm) showed that harder the ceramic, coarser were the fragments formed. On comparing the results with available armor systems, it has been concluded that TiB_2 based composites can show better ballistic properties, except B4C. SEM analysis of the fragments obtained after testing with FGM showed formation of cleavage steps as well as presence of intergranular cracks, indicating that the FGM fractured by mixed mode of failure. It can be concluded that the FGM developed has lower ballistic properties compared to its monolith TiB_2-20 wt.% *Ti*.

Keywords: TiB_2-*Ti* FGM, SPS, depth of penetration, ballistic efficiency, fractography

1. INTRODUCTION

The growing threats due to the increase in use of small calibre armor piercing projectiles are posing continuous threat to personnel on the battlefield. With the advancement in technology, newer explosives and explosive based projectiles have been introduced, which demand the development of new lightweight armor systems[1]. A good armor material must possess high hardness, elastic modulus, fracture toughness, compressive strength[2] and Hugoniot Elastic Limit (HEL). Also, the desired armor material should have multi-hit capability i.e. the material should be able to resist multiple bullets. The currently available body armor materials include ceramics, laminated composite structures and ballistic fabrics. Some of the structural ceramics as B_4C, SiC, Al_2O_3, aluminium nitride, TiB_2 and Syndie (synthetic diamond composite)[3-6] are considered as potential materials for armor applications for both personnel and vehicle protection, owing to their low density, reliability, superior hardness, compressive strength and greater energy absorption capacity, which enable effective erosion and defeat of the projectiles. These structural ceramics exhibit favorable properties such as high impact velocity for dwell/penetration transition and deformation induced hardening[7,8]. Therefore, as soon as the projectile hits the ceramic target, projectile gets shattered. If during impact the ceramic gets pulverized, the pulverized particles help in abrading the projectile further. However, ceramics being brittle usually lack multi-hit capability i.e. they cannot sustain successive impacts without quickly losing much of their strength property. Hence, they are susceptible to failure during service. Also, due to brittleness, when a projectile enters a ceramic, the entrance channel of the shaped projectile becomes ragged, as compared to that while penetrating a metal (ductile). The ragged channel cause asymmetric pressures and disturbs the geometry of the projectile[9]. The asymmetric pressures also cause great irregularities in the ceramic itself, leading to failure. Therefore, tougher composites need to be developed, which can cause effective crack deflection as well as lower projectile penetration by shattering, bending or change of path. Over the years, newer and tougher composites have been developed, which give about five times the protective value of the monolithic ceramics. These are usually metal matrix composites (MMCs), which have both ceramic and metal. Presently, B_4C and alumina are being frequently used in armor systems. But, these suffer from drawbacks such as, B_4C undergoes amorphisation at bullet speeds of 800-900 m/s and alumina has lower hardness and toughness. Therefore, there is a need to develop a new armor material system, which does not possess such disadvantages.

TiB_2 being a ceramic, is one of the good choices as armor material as it offers most of the required properties for being an armor material as high hardness, compressive strength, elastic modulus, HEL and ballistic efficiency. However, it possesses moderate fracture toughness, which is detrimental for its use as an armor material, as it cannot effectively resist the projectile penetration. Also, in order to attain near theoretical density,

Received 9 September 2012, revised 2 November 2012, online published 12 November 2012

high sintering temperatures (> 2100 °C) and long holding times are required using conventional sintering techniques[10-13]. Such extreme processing conditions adversely affect the mechanical properties as they result in abnormal grain growth[14-16]. Efforts have been made in the past to lower the sintering temperature by using various metallic binders (*Fe, Ni, Cr, Co, Ti*)[10,11,17]. Moreover, metals are best known for their toughness. We have chosen *Ti* as additive to TiB_2 to improve the toughness. *Ti* has similar density, crystal structure and coefficient of thermal expansion as TiB_2, and is therefore thermo-mechanically compatible with TiB_2. Also, *Ti* has lower melting temperature (1900 °C) compared to TiB_2, thereby allowing the densification of TiB_2 at lower temperatures via liquid phase sintering (LPS). Here, the toughness of the composite is expected to increase primarily due to crack deflection and ductile metal bridging. The *Ti*-rich phase hinders the crack propagation by the crack bridging based toughening mechanisms. Once initiated, the crack grows in the ceramic with plastically stretched metal grains behind the crack tip bridging the crack faces, thereby hindering the crack propagation.

The present armor design scheme consists of a hard face like ceramic to blunt or erode the projectile and is supported by a soft backing (usually metal)[18]. The hard face is expected to decelerate the projectile upon impact and the remaining fragments are being catched/stopped by the backing, which further reduces the projectile penetration into the target. This bilayered design can be achieved either by attaching the metal backing to the ceramic mechanically or by forming a functionally graded structure. Based on this, we tested a FGM design in which TiB_2 reinforced with 10 wt.% *Ti* phase is the hard face material and TiB_2 reinforced with 20 wt.% *Ti* phase is the backing material as shown in Fig. 1. The use of *Ti* introduced the appropriate toughness to TiB_2 and the FGM design allowed us to obtain the best material property. It is worthwhile to mention here that it is possible to fabricate FGMs by many conventional (casting, combustion synthesis, HP, HIP, other powder metallurgy processes) and novel methods (spark plasma sintering (SPS), plasma spraying, laser cladding). Amongst these, SPS is considered to be a suitable sintering technique for laminated and functionally graded composites, since SPS enables the sintering of the ceramic at lower temperatures and shorter duration. The shorter sintering times and lower sintering temperatures help in reducing the generation of residual stresses and pores in the gradient material. Also, SPS is a simple, cost effective and productive fabrication process and allows attainment of restricted grain size during sintering enabling one to achieve better mechanical properties[19]. The

Figure 1. FGM design scheme used in the present study.

graded structures can be produced by placing layers of powder mixtures in the die, such that the volume fraction of a specific phase constituent varies with each layer. But, it should always be kept in mind that the non-uniformity in property increases as the specimen size increases. In the present study, the gradient formation allowed us to achieve much higher hardness values (Hv ~ 41 GPa), using two stage spark plasma sintering (TSS), but with formation of a weaker interface (Hv ~ 28 GPa).

2. EXPERIMENTAL DETAILS

2.1 Materials Processing

Four different compositions for our study include monolith TiB_2, TiB_2-10 wt.% *Ti*, TiB_2-20 wt.% *Ti* composites and TiB_2-(10 wt.% *Ti*)/TiB_2-(20 wt.% *Ti*) based FGM. To obtain TiB_2-*Ti* compositions appropriate amounts of commercial TiB_2 (Grade NF, 1.9 μm, Japan New Metals Co. Ltd., Japan) and *Ti* (Goodfellow Cambridge Limited, 45 μm, UK) powders were mixed by wet ball milling for 24 h at 200 rpm in the presence of toluene as media in WC jars. The powder was then dried, crushed and then placed into a cylindrical graphite die of inner diameter 50 mm and height 70 mm, lined with graphite sheet. Then the graphite die containing the powder sample was placed inside the SPS chamber. The sintering of all the four compositions was carried out in the SPS apparatus [SPS-1080 (100kN, 8000A), Fuji Electronic Industrial Co., Ltd., Japan] in vacuum to the temperatures of 1500 °C - 2000 °C. All the samples were sintered via two stage sintering (TSS) to final sintering temperature of 1500 °C – 1600 °C at 50 MPa, except monolith TiB_2 which was sintered using single stage sintering to temperature of 2000 °C at 60 MPa pressure with 10 min hold (see Table 2). In the case of TSS, the powder compact was held for 5 min at a temperature of 1000 °C at 20 MPa pressure, so as to remove any volatile matter present. Subsequently, the powder compact was held at 1500 °C – 1600 °C for 6-8 min before turning off power at 50 MPa. After final stage of holding at sintering temperature, the power was turned off and the sample was allowed to cool naturally in the vacuum chamber. The rate of heating was kept constant as 60 °C/min throughout the sintering cycle. Here, the sintering temperature was monitored and regulated by an optical pyrometer, focused on the outer surface of the graphite die. The sintering behaviour was monitored by measuring the change in the axial dimension of the compact body. It is to be noted that the net heating time was kept constant for all the three composites viz. TiB_2-10 wt.% Ti, TiB_2-20 wt.% *Ti* composites and TiB_2-(10 wt.% *Ti*)/TiB_2-(20 wt.% *Ti*) FGM, so that comparative data can be obtained. After sintering, the composite samples except TiB_2, exhibited higher densities (>98%) and therefore, a comparison of their microstructure and mechanical properties is more rational to illustrate the influence of use of FGM as an armour material. A schematic representation of the sintering schedule followed in synthesizing TiB_2 and composite samples through SPS technique are presented in Fig. 2. It is to be noted that for these ballistic testing, 50 mm diameter dense TiB_2-based ceramic plates with 5 mm - 8 mm thickness were densified using commercial SPS machine. Such specimen size is much larger than the ceramic samples that are commonly sintered using SPS for research purpose in various research groups.

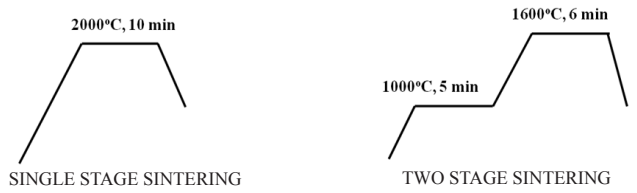

Figure 2. Schematic of sintering schedules used to obtain dense TiB_2-based ceramic armor plates.

2.2 Ballistic Testing

One of the evaluation techniques used to judge the ballistic performance of material against small-range projectiles is the determination of the ballistic efficiency by measuring the depth of penetration (DOP) of the projectile inside the metallic backplate material. DOP tests are performed using a set up shown in Fig. 3. The front portion of the target is a ceramic material, supported by a metal backing. A reference shot is fired into the reference backing and a second shot is fired on the candidate ceramic tile bonded to the same backing material (aluminium). Thereafter, the residual penetration depth into the reference backing material is compared. The major advantage of DOP test is its closeness to the desired armor applications. However, the problem is that each test gives a single number of residual penetration values.

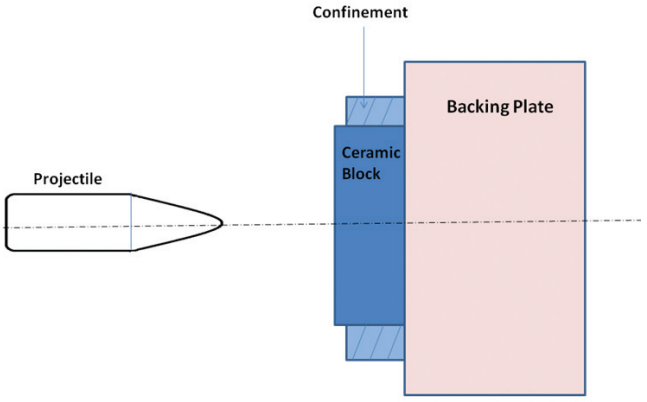

Figure 3. DOP test configuration, used in the present investigation.

The quantitative information for the test can be obtained from radiographs using X-ray technique. Based on such measurements, the ballistic property is reported in terms of ballistic efficiency (η) and is calculated using the following relationship:

$$\eta = (P_0\text{-}P_r)*D_0/t_c*D_c$$

where P_0 is reference penetration without ceramic layer, P_r is residual penetration of projectile (penetration with ceramic layer), D_0 is density of backing plate, D_c is density of ceramic, t_c is initial thickness of ceramic plate.

The ballistic testing was carried out on selected TiB_2 composites with the test parameters, as summarized in Table 1. The details of the sample preparation conditions and final sample size are provided in Table 2. All the samples were prepared using SPS and were fully dense except monolith TiB_2 (RD = 86.5%). A number of ceramic plates of circular cross

Table 1. Test parameters used for the ballistic testing of the selected TiB_2 composites

Test parameters	Dimension
Bullet size	7.6 mm diameter
Bullet material	hardened steel ($H_v > R_c$ 67)
Gun used	7.62 mm Dragunov
Bullet speed	≈ 820 m/sec (with full charge)
Firing distance	10 m
Confinement material	Steel
Backing material	Aluminum alloy 6063 -T6
Ammunition fired	7.62 AP
Angle of firing	Normal attack

Table 2. Summary of SPS sintering condition as well as ceramic plate dimensions used for ballistic testing as well as summary of ballistic results obtained with TiB_2-Ti based monolith/FGM

Specimen desig-nation	Ceramic composition	Specimen dimensions	Sintering conditions	Density (gm/cc)	Relative density (%)	Residual DOP in reference material (mm)	Ballistic efficiency (η)
S1	TiB_2-(10 wt.% Ti) / TiB_2-(20 wt.% Ti) (FGM)	ø= 50 mm, thickness = 5 mm	1000°C, 20 MPa, 5 min hold-1500°C, 50 MPa, 8 min hold	4.44	98.2	10	5.6
S2	TiB_2-(10 wt.% Ti) / TiB_2-(20 wt.% Ti) (FGM)	ø= 50 mm, thickness = 5 mm	1000°C, 20 MPa, 5 min hold-1600°C, 50 MPa, 6 min hold	4.50	99.3	14	5.1
S3	TiB_2-(10 wt.% Ti)	ø= 50 mm, thickness = 5 mm	1000°C, 20 MPa, 5 min hold-1600°C, 50 MPa, 6 min hold	4.48	98.8	11	5.4
S4	TiB_2-(20 wt.% Ti)	ø= 50 mm, thickness = 5 mm	1000°C, 20 MPa, 5 min hold-1600°C, 50 MPa, 6 min hold	4.50	99.5	11.5	5.4
S5	TiB_2 (Monolithic)	ø= 40 mm, thickness = 6.1 mm	2000°C, 60 MPa, 10 min hold	3.92	86.5	4	5.9
S6	TiB_2-(10 wt.% Ti) / TiB_2-(20 wt.% Ti) (FGM)	ø= 50 mm, thickness = 7.8 mm	1000°C, 20 MPa, 5 min hold-1600°C, 50 MPa, 6 min hold	4.53	99.9	2.5	4.1

* Reference penetration in Al alloy = 56 mm

section with 5 mm - 8 mm thickness are supported by steel clamp with Aluminium back plate and the details are provided in Table 2. After tests, the cross-section of *Al*-backplate is investigated to measure residual depth of penetration produced by the bullet using x-ray radiography and based on such measurements, the ballistic efficiency is measured. After the ballistic testing, the fragment sizes of the fractured ceramic plates are measured using Scanning electron microscopy (SEM) and in case of larger fracture surfaces, the characteristics of fracture were also studied using SEM.

3. RESULTS AND DISCUSSION

3.1 Ballistic Efficiency of TiB_2-*Ti* FGM

After the ballistic testing, the following evaluations were performed to analyse the tested material in the context of armor applications. These provided us with an indication of energy absorbed via studying the following aspects:

(a) Fracture surfaces of shattered ceramic discs.
(b) Fracture surfaces of shattered bullets.
(c) Sieve analysis/fragment size analysis of fractured ceramic pieces.

The ballistic efficiencies determined for different TiB_2 composites are summarized in Table 2. It is found that all the tested ceramic compositions exhibit the ballistic efficiency, η = 5.1 – 5.9, except for the FGM plate with thickness = 7.8 mm. This indicates that by increasing the thickness for FGM from 5 mm to 7.8 mm, does not contribute towards improvement in the ballistic property of the material. One important aspect, which was noted during the ballistic tests conducted on TiB_2-based materials, is that after each impact, the projectile used was completely shattered into fine pieces. This indicated that we can achieve complete stoppage of the projectile, by refining our present armor design scheme. We have compared our results with other available armor systems in Table 3. Comparing the data in Table 3, it is clear that TiB_2-based ceramic systems have lower depth of penetration and higher ballistic efficiencies compared to other ceramic armor systems, except B_4C[20]. It should be noted that the type of projectile used (pointed/blunt) strongly influences the final ballistic efficiency. The pointed projectile imparts more damage to the target. For example, under identical ballistic test conditions, the pointed and blunt projectiles leave depth of penetration of 200 mm and 46 mm respectively for glass armor, while the respective numbers for ZrO_2 are 68 mm and 42 mm. It is interesting to note, monolithic TiB_2 (without any reinforcement) despite having density of less than 90% ρ_{th} (theoretical density), has extremely low DOP and higher ballistic efficiency (η) than TiB_2-$MoSi_2$ composites, which have more than 99% ρ_{th}. This can be explained by hard TiB_2 grains being resistant to high impact projectile and the absence of any weak interface (e.g. $TiB_2/MoSi_2$), which provides easier path for crack propagation.

We have also investigated the size of the fragments of the shattered ceramics, obtained after the ballistic test and the results obtained are presented in Fig. 4. If we compare the three single compositions viz. monolith TiB_2, TiB_2-(10 wt.% Ti) and TiB_2-(20 wt.% Ti), the following observations can be drawn:

(a) for monolith TiB_2, the fragment size varies from 2.4 μm to 18 mm.

Table 3. Comparison in ballistic properties of TiB_2-*Ti* compositions studied with different ceramic armor materials.

Material	Depth of Penetration (mm)	Ballistic Efficiency (η)
*Aluminum (pointed)	265	--
*Aluminum (blunt)	75	--
*Glass (pointed)	200	4.2
*Glass (blunt)	46	1.6
*Alumina 85 (pointed)	122	8.6
*Alumina 995 (pointed)	50	11.7
*Zirconia (pointed)	68	9.3
*Zirconia (blunt)	42	1.3
*TiB_2 (Ceradyne, pointed)	38	11.1
**TiB_2 -2.5% $MoSi_2$ (pointed)	11	5.1
**TiB_2 -10% $MoSi_2$ (pointed)	11	5.1
# TiB_2 (86.5% ρ_{th}, pointed)	4	5.9
# TiB_2-(10 wt.% *Ti*) (98.8% ρ_{th}, pointed)	11	5.4
# TiB_2-(20 wt.% *Ti*) (99.5% ρ_{th}, pointed)	11.5	5.4
# TiB_2-(10 wt.% *Ti*)/TiB_2-(20 wt.% *Ti*) (98.2% ρ_{th}, pointed)	10	5.6
# TiB_2-(10 wt.% *Ti*)/TiB_2-(20 wt.% *Ti*) (99.9% ρ_{th}, 8mm, pointed)	2.5	4.1
B_4C[20]	4-18	--

Note: The relative density values of the TiB_2-based materials % ρ_{th}, where ρ_{th} = theoretical density, are mentioned within parenthesis. Also, the use of pointed/blunt type of projectile used for ballistic testing has been mentioned.

*: Results by Woodward[21] *et al.* (Note: Reference penetration into 2024 T351 Al alloy = 265 mm, projectile used: 7.72 mm W-alloy).
**: Raju[22] *et al.*
#: present work (Note: Reference penetration into 6063 T6 *Al* alloy = 56 mm, projectile used: 7.62 mm hardened steel $H_v > R_c$ 67).

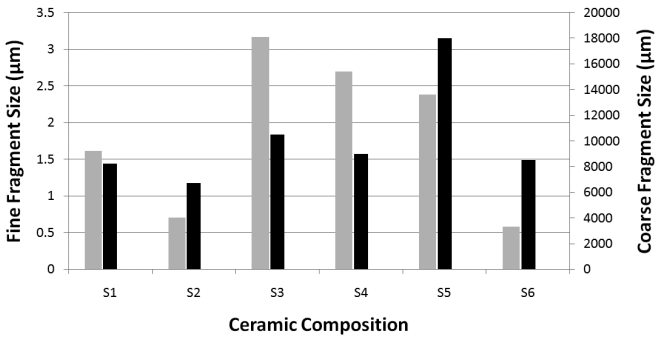

Figure 4. Comparison in ceramic fragment size obtained after ballistic testing of the TiB_2- based ceramic armors, investigated in the present study (For ceramic sample designation, see Table 2).

(b) for TiB_2-(10 wt.% *Ti*), the size varies from 3.2 μm to 10.5 mm, and

(c) for TiB_2-(20 wt.% *Ti*), the size varies from 2.7 μm to 9 mm.

The monolith TiB_2, being the hardest among the three compositions, exhibits the coarsest fragment size, while TiB_2-(10 wt.% *Ti*), being harder than TiB_2-(20 wt.% *Ti*) show coarser fragment size compared with TiB_2-(20 wt.% *Ti*). This clearly indicates that harder is the material, coarser the fragments obtained. From Table 2, it can be seen that S1 and S2 samples have thickness 5 mm, but sample 2 is more dense than sample 1 and S6 have a thickness of 7.8 mm. After the ballistic test, the fragment size from S1 sample varies from 1.6 μm to 8.2 mm, for S2 sample, it is from 0.7 μm to 6.7 mm and for S6 sample, size varies from 0.6 μm to 8.5mm. From the above, it can be concluded that the most dense ceramic of 5 mm thickness (S2) show the finest fragments compared to others. This implies that denser that ceramic, finer is the fragment size.

From Fig. 4, it also can be seen that more coarser particles were recorded after ballistic testing with monolithic TiB_2 compared to the composites, while more finer particles in case of TiB_2-(10 wt.% Ti)/TiB_2-(20 wt.% Ti) layered FGM discs. This is an advantage against monolithic TiB_2. When a bullet impacts TiB_2-(10 wt.% Ti)/TiB_2-(20 wt.% Ti) FGM, more impact energy is absorbed by the material, thereby forming fine fragments. This further helps in stopping the bullet penetration. This mechanism can be explained with the help of Fig. 5. In Fig. 5(a), as soon as the projectile hits the target, the material gets cracked and the crack is propagated in such a manner that larger chunks of material are removed i.e. the total crack path taken is smaller. On the other hand in Fig. 5(b), a larger crack path is followed. This means that more projectile energy is being absorbed by the target in the second case. Hence, it is believed that the later scenario improves the ballistic property. In the published literature, rarely studies could be found, which reported such kind of fragment analysis to show the appropriateness of their material for ballistic impact resistance.

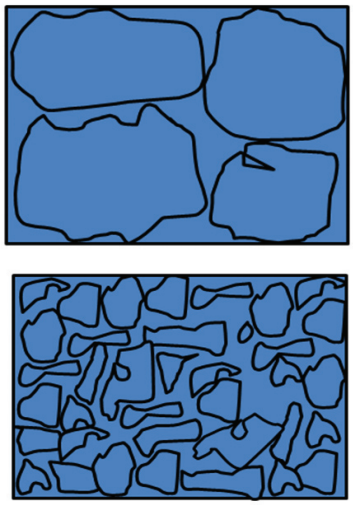

Figure 5. Schematic illustration of the two mechanistic descriptions, illustrating the bullet impact induced cracking in the target material (a) small crack path, (b) larger crack path.

3.2 Ballistic Impact Induced Fracture Behaviour

To obtain a complete understanding of the fracture mode due to impact failure, we have carried out SEM fractographic study on the ceramic fragments, obtained after the ballistic test. Secondary electron mode (SE-SEM) images of fractured surfaces of the compositions ballistically tested were taken and are shown in Fig. 6. A closer observation of Figs. 6(a)-(c) helps us to summarize the following observations:

(a) TiB_2-(10 wt.% *Ti*) composite predominantly failed by intergranular mode of fracture (see Fig. 6(a)).

(b) TiB_2-(20 wt.% *Ti*) composite predominantly failed by transgranular mode of fracture (see Fig. 6(b)).

(c) TiB_2-(10 wt.% *Ti*)/TiB_2-(20 wt.% *Ti*) FGM failed by mixed mode of fracture (see Fig. 6(c)). Cleavage steps, which are typical features of transgranular fracture, can be clearly seen.

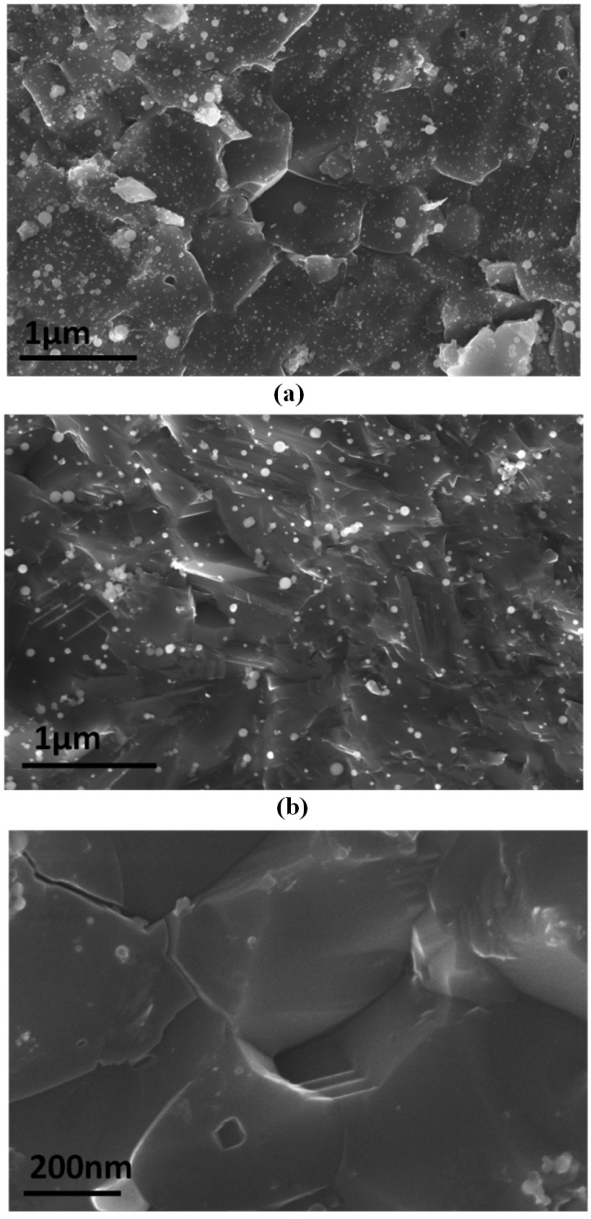

Figure 6. SEM fractographs after ballistic testing for (a) TiB_2-10 wt.% *Ti* composite, (b) TiB_2-20 wt.% *Ti*, and (c) TiB_2-(10 wt.% *Ti*)/TiB_2-(20 wt.% *Ti*) FGM discs.

The above observations indicate that FGM has lower strength compared to its monolith counterpart, TiB_2-(20 wt.% *Ti*). This can be attributed to the presence of a weaker interface between TiB_2-(10 wt.% Ti) and TiB_2-(20 wt.% *Ti*) sides of the FGM, having lower strength. Although, with Ti addition, we have not achieved any improvement in the ballistic property of TiB_2, nevertheless we were able to achieve fully dense composites having similar properties of monolith TiB_2 at lower production costs. Also, in our study, the ceramic strength is found to be sufficient, so as to completely fracture the nose of the pointed projectile used. Moreover, TiB_2 has higher density due to which it is more applicable for longer arms (like tanks) and not for body armors, due to the heavy weight involved. Ti addition allowed lowering of the overall weight of the component, thereby allowing the use of TiB_2 for protection against smaller arms.

We have also carried out SEM fractographic study on the shattered ceramic samples of TiB_2-$MoSi_2$[14] composites after the ballistic testing and some representative SEM images of fractured surfaces after ballistic testing are shown in Fig. 7 and Fig. 8, respectively. A closer observation of Figs. 7(a) - 7(d), reveals the following distinctive features in case of TiB_2-2.5%$MoSi_2$:

(a) The fracture mode is predominantly transgranular in nature with extensive crack propagation along the cleavage planes,

(b) The fracture steps or, striations are observed in many grains.

The characteristic presence of multiple parallel fracture planes, like a deck of cards, is observed on many of the TiB_2 grains in case of TiB_2-$MoSi_2$ material. With increase in $MoSi_2$ addition from 2.5 to 10 wt. %, the predominant fracture mode changes from transgramular to intergranular mode (see Figs. 8(a) - 8(c). This characteristic damage as well as fracture striations are also observed on dynamically fractured surfaces of TiB_2-*Ti* composites (Fig. 6(c)).

4. COMPARISON WITH OTHER CERAMIC ARMORS

In earlier research from our group, TiB_2-2.5 wt.% $MoSi_2$ and TiB_2-10 wt.% $MoSi_2$ compositions were prepared using hot pressing and the ballistic studies of the material were conducted to have a comparison of the ballistic efficiency of various TiB_2-based materials. It was found that the addition of $MoSi_2$ to TiB_2 has resulted in a decrease in ballistic efficiency. More precisely, in case of monolithic TiB_2, one can obtain ballistic efficiency of ~ 6 (see Table 3). However, after the addition of 2.5% $MoSi_2$ and 10% $MoSi_2$ to TiB_2, we get ballistic efficiency only ~5-5.2.

A comparison of the present results with those obtained with available armor material systems is summarized in Table 3. Woodward [21], *et al.* studied the ballistic property by making ceramic tiles of 100 mm square with 12.7 mm thickness backed with a 6.35 mm thick 2024 T351 aluminium backing and surrounded by a steel jacket. For the samples studied, they found that the less tough ceramics form more fragments compared to tougher ceramics. Similar observations were made in our current study that harder the material, coarser are the fragments obtained after ballistic testing. A careful observation of the ballistic efficiency results (Table 3) show

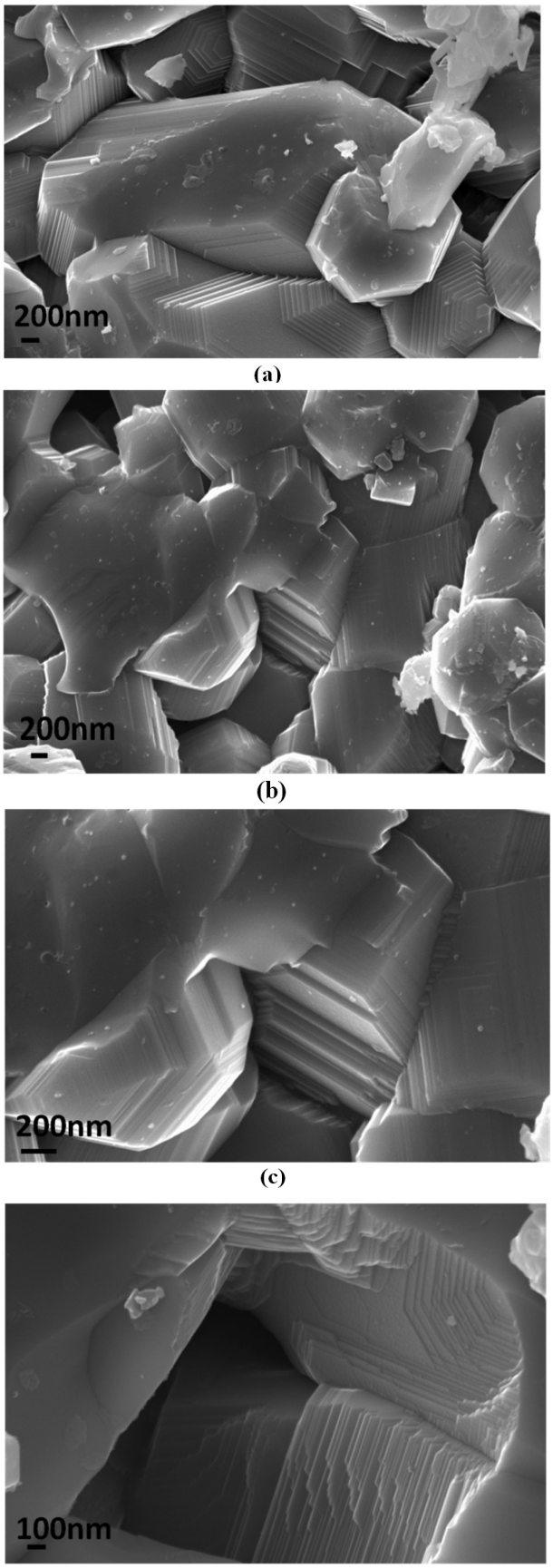

Figure 7. Representative SEM images revealing the overall morphology (a), (b) and details revealing the cleavage steps on fractured particles of TiB_2-2.5%$MoSi_2$ after ballistic testing (c), (d).

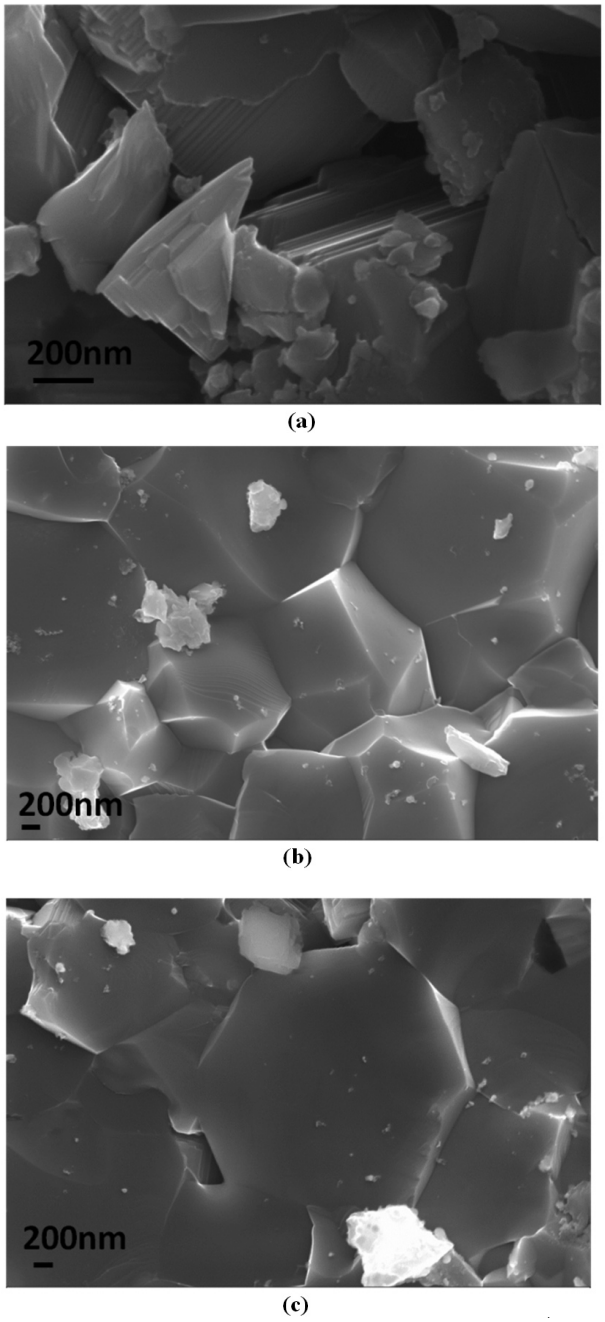

Figure 8. Representative SEM images revealing the overall intergranular morphology and details revealing the cleavage steps on fractured particles of TiB_2-10%$MoSi_2$ after ballistic testing (a)-(c).

that metal aluminium showed the maximum DOP and the ballistic efficiency of oxide ceramics (glass, aluminia: AD85, AD995 and zirconia) is lower compared to borides (TiB_2 and its composites) and carbides (B_4C). All such observations together indicate that borides and carbides are good choices as far as armor applications are concerned.

5. CONCLUSIONS

Based on the experimental results presented and analysed in this paper, following conclusions can be drawn:

- The ballistic tests with hardened steel bullets at high velocity (~ 820 m/s) normal impact leads to the complete shattering of the spark plasma sintered TiB_2-Ti based composites and FGM armor plates having 50 mm diameter and 5 mm-8 mm thickness. An extensive analysis of the fragments reveals the size distribution of around 2-10,000 μm with little larger fragments measured with monolith TiB_2 (~ 2 μm – 18 mm).
- In terms of estimation of the ballistic efficiency (η), the values of η determined from depth of penetration tests revealed a small variation (5.1-5.9) in all the TiB_2-based ceramic compositions. The values of the ballistic efficiency (η) measured are still lower than the reported values of B_4C. To further increase the value of η, innovative design concepts in TiB_2-Ti need to be considered in future studies.
- In terms of crack propagation during the high velocity impact, TiB_2-Ti based FGM failed via mixed mode of fracture, while TiB_2-20 wt.% Ti composite predominantly failed via transgranular fracture. It is worthwhile to mention that TiB_2-$MoSi_2$ composites, tested under similar impact conditions, fail via transgranular fracture with multiple parallel cleavage planes in TiB_2 grains.

ACKNOWLEDGEMENTS

The authors thank Department of Science and Technology, India; Defence Research and Development Organisation, India; to procure SPS facility at IIT Kanpur. We thank Director DMRL, Hyderabad, India for allowing ballistic tests on the samples. We also thank Dr T. Mori at National Institute of Material Science, Tsukuba, Japan; for the SPS facility.

REFERENCES

1. Weinong, W.; Chen, A.M.; Rajendran; Song, Bo & Nie, Xu. Dynamic fracture of ceramics in armor applications. *J. Am. Ceram. Soc.,* 2007, **90** (4), 1005-018.
2. Basu, B. & Balani, K. Advanced structural ceramics. USA and American Ceramic Society, John Wiley & Sons, Inc., 2011.
3. Tarry, United States Patent [19], Patent no. 5443917, 22 Aug 1995.
4. Homlmquist, T.J.; Rajendran, A.M.; Templeton, D.W. & Bishnoi, K.D. A ceramic armor database. TARDEC Technical Report, Jan 1999.
5. Kumar, K.S. & DiPietro, M.S. Ballistic penetration response of intermetallic matrix composites. *Scripta Metallurgica et Materialia*, 1995, **31**(5), 793-98.
6. Madhu, Vemuri; Ramanjaneyulu, K.; Bhat, T. Balakrishna & Gupta, N.K. An experimental study of penetration resistance of ceramic armour subjected to projectile impact. *Int. J. Impact Eng.,* 2005, **32**(1-2), 337-50.
7. Lundberg, P.; Renstrom, R. & Lundberg, B. Impact of metallic projectiles on ceramic targets:transition between interface defeat and penetration. *Int. J. Impact Eng.,* 2000, **24** (3), 259-275.
8. Qiao, Pizhong; Yang, Mijia & Bobaru, Florin. Impact mechanics and high-energy absorbing materials: Review. *J. Aerospace Eng.,* 2008, **21**(4), 235-48.
9. http://www.martinfrost.ws/htmlfiles/june2008/chobham_armour.html

10. Basu, B. Raju, G.B. & Suri, A.K. Processing and properties of monolithic TiB_2 based materials. *Int. Materials Rev.*, 2006, **51**(6), 352-74.
11. Baik, S. & Becher, P.K. Effect of oxygen contamination on densification of TiB_2. *J. Am. Ceram. Soc.*, 1987, **70**(8), 527-30.
12. Ch.Murthy, T.S.R.; Basu, B.; Balasubramaniam, R.; Suri, A.K.; Subramanian C. & Fotedar, R.K. Processing and properties of TiB_2 with $MoSi_2$ sinter-additive: a first report, *J. Am. Ceram. Soc.,* 2006, **89**(1), 131-38.
13. Wang, W.; Fu, Z.; Wang, H. & Yuan, R. Influence of hot pressing sintering temperature and time on microstructure and mechanical properties of TiB_2 ceramics. *J. Eur. Ceram. Soc.*, 2002, **22**, 1045-049.
14. Ferber, M.K.; Becher, P.F. & Finch, C.B. Effect of microstructure on the properties of TiB_2 ceramics. *J. Am. Ceram. Soc.,* 1983, **66**(1), C2-4.
15. Zhang, Z.H.; Wang, F.C.; Wang, L. & Li, S.K. Ultrafine-grained copper prepared by spark plasma sintering process. *Mater. Sci. Eng.* A, 2008, **476**(1-2), 201-05.
16. Zhang, Z.H.; Wang, F.C.; Lee, S.K.; Liu, Y.; Cheng, J.W. & Liang, Y. Microstructure characteristic, mechanical properties and sintering mechanism of nanocystalline copper obtained by SPS process. *Mater. Sci. Eng. A*, 2009, **523**(1-2), 134-38.
17. Telle, R. Boride and carbide ceramics, structure and properties of ceramics, Materials Science and Technology, edited by R.W. Cahn, P. Haasen, and E.J. Kramer. Swain VCH, Weinheim, Germany, 1994, **11**, 175.
18. Chin, E.S.C. Army focused research team on functionally graded armor composites. *Material Sci. and Eng.*, 1999, **A259,** 155-61.
19. Gupta, Neha; Mukhopadhyay, Amartya; Pavani, K. & Basu, Bikramjit. Spark plasma sintering of novel ZrB_2 - SiC - $TiSi_2$ composites with better mechanical properties. *Materials Sci. Eng. A*, 2012, **534**, 111-18.
20. Savio, S.G.; Ramanjaneyulu, K.; Madhu, V. & Bhat, T. Balakrishna. An experimental study on ballistic performance of boron carbide tiles. *Int. J. Impact Eng.,* 2011, **38**(7), 535-41.
21. Woodward, R.L.; Gooch Jr., W.A.; O'Donnell, R.G.; Perciballi, W.J.; Baxter B.J. & Pattie, S.D. A study of fragmentation in the ballistic impact of ceramics. *Int. J. Impact Eng.,*1994, **15**(5), 605-18.
22. Raju, G.B. & Basu, B. Influence of $MoSi_2$ addition on load-dependent fretting wear properties of TiB_2 against cemented carbide. *J. Am. Ceram. Soc.,* 2009, **92**(9), 2059-066.

Contributors

Ms Neha Gupta obtained her undergraduate and postgraduate degrees, both in Materials Science in Engineering from Punjab Technical University, Jalandhar and Thapar University, Patiala (Punjab) in 2005 and 2007, respectively. is a research scholar at Department of Materials Science and Engineering, Indian Institute of Technology Kanpur (IITK) since January 2010. She also worked as Assistant Manager at Trident (Process & Quality Control) for more than two years and at MEMS Lab, Department of Mechanical Engineering, Indian Institute of Science, Bangalore for four months.

Dr Velidandla Venkata Bhanu Prasad obtained his PhD in Powder Metallurgy from the Indian Institute of Technology (IIT) Bombay. He is presently working as Scientist 'G' at the Defence Metallurgical Research Laboratory (DMRL), Hyderabad. He heads the Ceramics and Composites Group and works in the area of development of various types of ceramics and ceramic matrix composites for defence applications. He is a recipient of the Andhra Pradesh Scientist Award in the Year 2005 and DMRL Technology Group Award (as team leader) in 2010. He has more than 60 research papers and technical publications to his credit. His research interests are in the area of Aluminium and Titanium Matrix composites, Reaction Bonded Silicon Carbide (RBSC) and Boron carbide (RBBC), synthesis and consolidation of Ultra High Temperature Ceramics (UHTCs) and C_f-C-SiC & C_f-SiC composites for defence applications.

Dr Vemuri Madhu obtained his PhD in Applied Mechanics from the Indian Institute of Technology (IIT) Delhi. He also worked as a Postdoctoral Research Fellow at University of California, Los Angeles, USA. He is presently working as Scientist 'G' at the Defence Metallurgical Research Laboratory(DMRL), Hyderabad. He heads the composite armour design and development group and works in the areas of development of ceramic and composite armour materials and systems for various types of protective platforms. He is a recipient of the DRDO Performance Excellence Award in 2008 (as a team member), Laboratory Scientist of the Year Award in 2006 and National Technology Day Award in 2003. He has more than 50 research papers and technical publications to his credit. His research interests are in the areas of ceramic and composite armour development, modelling and simulation of ballistic phenomena, high strain rate characterisation of materials, shock and blast studies on armour materials and development of protective systems for military and civil applications.

Dr Bikramjit Basu obtained his PhD in Ceramics at Katholieke Universiteit Leuven, Belgium in March, 2001.Presently working as a Professor at Indian Institute of Technology (IIT), Kanpur. In recognition of contributions to the field of ceramic science and biomaterials science, received noteworthy awards from Indian Ceramic Society (2003), Indian National Academy of Engineering (2004), Indian National Science Academy (2005), Coble Award for Young Scholars (2008), Metallurgist of the year award (2010), NASI - SCOPUS Young Scientist Award (2010) and Materials Research Society of India (MRSI) Medal (2011). He has authored/co-authored more than 175 peer-reviewed research papers. He edited a book on Biomaterials, and authored two textbooks -Structural Ceramics and Tribology.